photonics

MDPI

Article

Experimental Investigation on the Performances of Innovative PV Vertical Structures

Gianluca Acciari *, Gabriele Adamo, Guido Ala, Alessandro Busacca, Massimo Caruso, Graziella Giglia, Antonino Imburgia, Patrizia Livreri, Rosario Miceli, Antonino Parisi, Filippo Pellitteri, Riccardo Pernice, Pietro Romano, Giuseppe Schettino and Fabio Viola

Dipartimento di Ingegneria, Università degli Studi di Palermo, 90128 Palermo, Italy

* Correspondence: gianluca.acciari@unipa.it

Received: 23 May 2019; Accepted: 25 July 2019; Published: 31 July 2019

Abstract: The sustainable development of our planet is considerably related to a relevant reduction of CO_2 global emissions, with building consumption contributing more than 40%. In this scenario, new technological conceptions, such as building-integrated photovoltaic technology, emerged in order to satisfy the requirements of sustainability imposed by the European Union. Therefore, the aim of this work is to provide a technical and economical comparison of the performances of different vertical-mounted innovative photovoltaic systems, potentially integrated on a building instead of on traditional windows or glass walls. The proposed investigation was carried out by means of experimental tests on three different next-generation vertical structures. The related results are described and discussed, highlighting the advantages and the drawbacks of the proposed technologies.

Keywords: photovoltaic technology; dye-sensitized solar cell; BIPV (building-integrated photovoltaic) technology

1. Introduction

Currently, building consumption contributes to more than 40% of CO_2 emissions, which are mainly caused by heating, air conditioning, and power systems in general. Therefore, the improvement of the performances of such systems represents a relevant aspect that needs to be taken into account toward the sustainable development of our planet, reducing the global emissions by up to 80% by the year 2050, according to the requirements imposed by the European Union (EU) [1–3].

In this scenario, buildings should be refurbished and technologically improved in order to optimize their energy efficiency and sustainability. Typically, this can be achieved by means of two main methodologies: passive methods, finalized to reduce the energy demand in terms of both cooling and heating, and active methods, which are focused on the development of innovative active and green technologies integrated into the building, capable of generating electrical energy in a sustainable way. For instance, the replacement of traditional windows or glass walls with renewable energy systems, such as photovoltaic (PV) innovative structures, could provide a significant reduction in terms of energy consumption of the building [4–6]. The third-generation PV systems, namely dye-sensitized solar cells (DSSC), are suitable for architectural integration [7,8]. Moreover, due to their bifacial features, the DSSC cells can replace glass windows, converting the light of both the indoor and outdoor environments [9,10].

In this context, this work presents a technical and economical comparison of the performances of different vertical-mounted innovative and integrated photovoltaic systems. Section 2 further describes the current background concerning building-integrated PV technology.

The experimental investigation is extended for the DSSC and thin-film silicon technologies, reported in Section 3. Section 3 also describes the experimental set-up employed to evaluate the

performances of the classes of cells considered. The technical and economical performance comparisons in terms of cost, efficiency, and fill factor are discussed in Sections 4 and 5.

2. Building-Integrated Photovoltaic Technology

Due to the mandatory requirement for a global reduction of pollutants, zero-energy and self-powered buildings represent an attractive solution in future urban scenarios. Therefore, BIPV (building-integrated photovoltaic) technology was increasingly developed in the last few years. The main idea of this technological solution is the adoption of PV materials in place of the bulky structural elements conventionally presented by buildings. Non-integrated PV systems are, therefore, likely to be soon overtaken by BIPV systems, due to the double role played by this innovative solution. Indeed, BIPV technology can be employed both as a building material and as a power generator, thus avoiding additional space for PV module installation. The description of PV technology's evolution and its respective use for building integration is provided in Sections 2.1–2.3.

2.1. The First Generation of Solar Cell Technology in BIPV Systems

Single-junction cells based on silicon wafers represent the first generation of solar cells developed for BIPV systems. This technology consists of crystalline silicon (c-Si) structures, which are roughly and rigidly placed on the building's roof, as shown in Figure 1. They are generally characterized by the following aspects: high thickness (0.2–0.5 mm), which clashes with architectural integration; a 10–16% efficiency range, guaranteed from 20 to 30 years, which gained attention in a period of low cost of electrical energy; very solid know-how, due to its commercial spread since the 1970s; overall approximate cost of 3000–4500 €/kWp installed, which requires an incentive policy for its diffusion.

(**a**) (**b**)

Figure 1. Some examples of building-integrated photovoltaic (BIPV) systems on buildings: (**a**) country house; (**b**) modern building.

The polycrystalline silicon (poly-Si) technology was thereafter developed to reduce the associated costs. Despite the novelty represented by the upgraded technology in the purification process of poly-Si (metallurgical material in place of a chemical one), the PV modules based on this material are not perfectly suitable for building integration due to their non-uniform tonality.

2.2. The Second Generation of Solar Cell Technology in BIPV Systems

The second generation PV technology presents single junction devices, employing amorphous silicon (a-Si), polycrystalline-Si (p-Si), copper indium gallium diselenide (CIGS), cadmium telluride/cadmium sulphide (CdTe/CdS), or deposited on low-cost substrates, such as glass. CdTe, CIGS and a-Si feature a higher solar spectrum absorption with respect to that of c-Si and poly-Si, so that an active material reduction is possible at the same efficiency as that of first generation solar cells.

Therefore, second generation BIPV panels are more flexible than first generation ones, featuring the following aspects: low thickness (10–100 μm); integration is no longer a sum of dissimilar elements;

a 6–10%, efficiency range guaranteed from 15 to 20 years; in spite of an efficiency reduction, the use of larger surfaces, allows compensation even though with a lower visual impact; consolidated know-how, due to a commercialization for over fifteen years; high level of consumer confidence.

The low-cost metallurgical process remarkably contributed to cost reduction, especially for high volumes of cells, as highlighted in Figure 2, where the price of installed cells as a function of their number is reported, for the two solar cell generations. It is well known that the second generation is introduced at the inflection point of the first one.

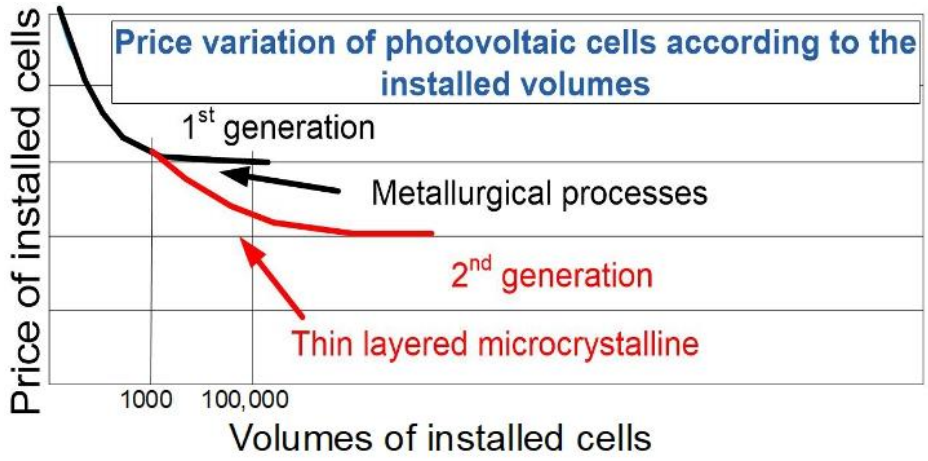

Figure 2. Cost reduction for second generation photovoltaic (PV): the low-cost metallurgical processes contribute to the realization of more cells.

By depositing onto a substrate several layers of photovoltaic solar cell materials, an a-Si thin film is obtained. This deposition can occur at temperature values which are low enough to be also compliant with plastic supports, so that bent structures can be realized, as the one shown in Figure 3.

Figure 3. Example of bent structure based on the second generation PV.

2.3. The Third Generation of Solar Cell Technology in BIPV Systems

The BIPV systems of the third generation are characterized by the same deposition and thin-film processes used for the second generation cells. Nevertheless, manufacturing costs are decreased by opting for low-cost non-toxic materials and by increasing the active materials surface. This technology is characterized by the following aspects: a theoretically obtainable efficiency of around 25%; adoption of inorganic materials presumably used.

Figure 4 highlights the goal of the third generation PV: in order to increase the spread of generation systems, by the conversion of each surface into an improved surface, price reduction should lead to increase the occupied area. It can be noted that the third generation is introduced at the inflection point of the second one.

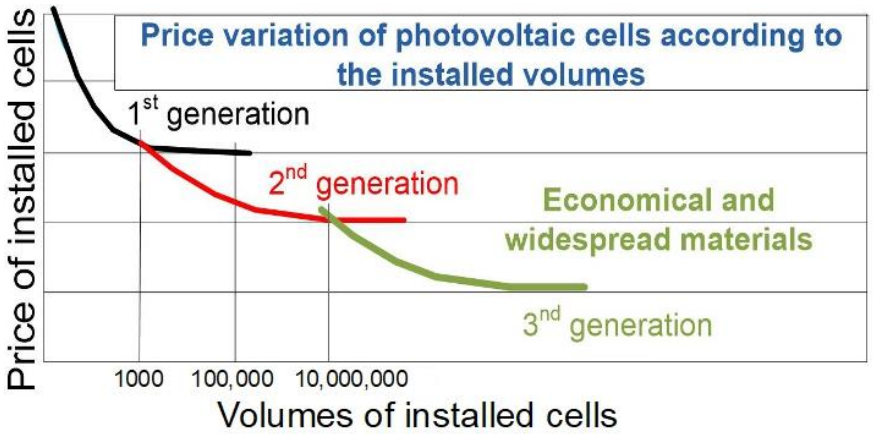

Figure 4. Cost reduction for the third generation PV.

2.3.1. DSSC (Dye-Sensitized Solar Cells)

The DSSC (dye-sensitized solar cell) is a solar cell featuring low cost and belonging to the family of thin film solar cells, conceived in 1991 by Brian O'Regan and Michael Gratzel [7]. The features of this technology can be summarized as follows: semi-flexibility and semi-transparency, which allow high integration levels; adoption of low-cost materials, which are abundant in nature; short-circuit current density, namely Jsc, almost equal to 20 mA/cm^2; open circuit voltage, namely V_{oc}, equal to 0.7 V; efficiency in the range between 10–12%, values traditionally used; stability up to 60–65 °C, which can be limiting in some applications; suitable for low-cost and high-volume production; more than 20% expected efficiency over 5–10 years; good results even with diffused light. The principle of operation for a DSSC cell is schematically represented in Figure 5.

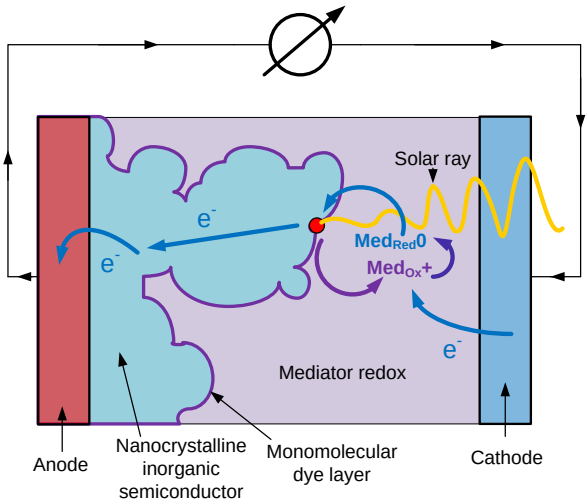

Figure 5. Operation of a dye-sensitized solar cell (DSSC).

A nanocrystalline material of inorganic semiconductor is deposited on a transparent electrode and covered with an organic layer of monomolecular dye. All these materials are immersed in an electrolyte liquid, in which a mediator of oxidoreduction is dissolved.

A dye of organic material generates an excited state (electron + hole), whenever hit by the sun's radiation; the electron is led to the inorganic semiconductor conduction band, while the hole stays on the dye. The mediator gives the electron which is missing in the dye and therefore it is oxidized. The electron that was directed to the semiconductor arrives at the anode and at the electric circuit to supply the load. An electron closes the circuit flowing from the cathode to reduce the oxidized mediator.

The DSSCs dye can feature different colors to guarantee a proper integration with the architectural structure. Further details on characterization and modelling carried out on DSSC cells can be found in [11–16]. In order to provide a good comparison among the different PV systems, the Green's tables should be considered. The mean performances such as efficiency, fill factor and open circuit voltage are reported [17].

2.3.2. BIPV Structures

Several structures are allowed by the use of third generation PVs, such as foil, tile, module and solar glazing. Foil products are notably lightweight, flexible and particularly suitable for being placed on the roofs. Tiles can be successfully employed to partially or totally cover the roof. Thanks to flexibility and chromatic variability provided by third generation PV modules, appreciable results in terms of geometries and colors can be achieved by the use of these tiles.

Due to several levels of color and transparency offered by the PV cell glazing products, an unrestricted selection of solutions for windows, facades, glassed and roofs is possible, so that the targets in terms of both energy production and aesthetics can be reached. Furthermore, the PV cell glazing modules spread the sunlight and provide protection from natural elements like a conventional window. Figure 6 shows some examples of the different products.

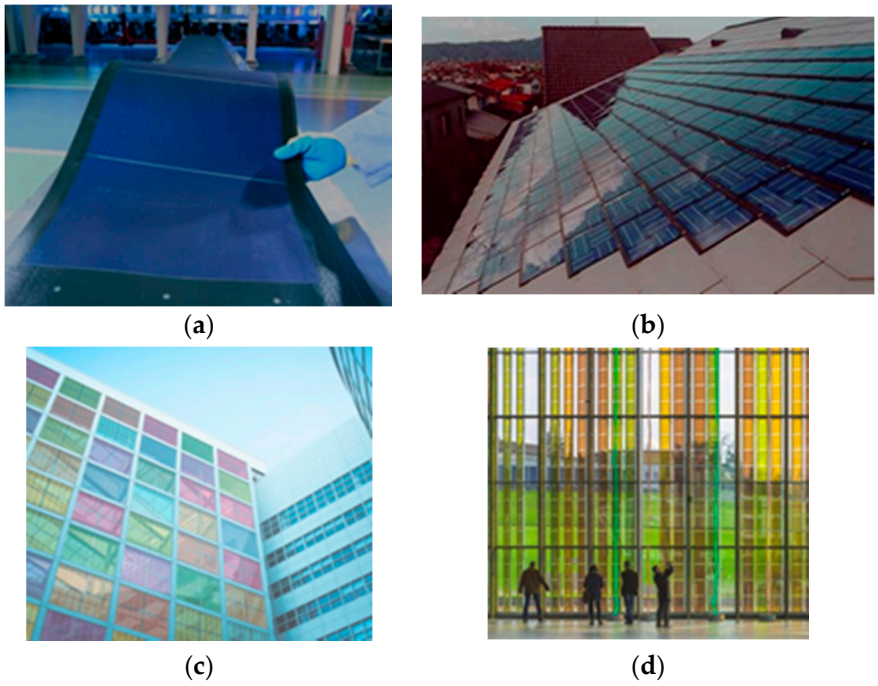

Figure 6. Third generation BIPV products: (**a**) foil; (**b**) tiles; (**c**) module on façade; (**d**) solar glazing.

3. Experimental Setup

As introduced in the previous Sections, PV vertical structures have a triple aim: production of electrical energy, transmission of light in the building and regulation of heat transmission. The use of technology is the filament connecting these different pieces. The introduction of an electrical power generation surface actually changes the transmittance properties of the window, for both light radiation and heat transfer.

The realization of shading solution can be achieved by integrating semi-transparent modules inside a glass shell. In order to maximize both energy savings and generation of electrical energy, transparency should be accurately balanced, as reported in [18–20].

The vertical structures compared in this work are shown (during their installation) in Figure 7; the location is University of Palermo, Italy. With regards to the DSSC panel, 8 modules (30 × 30 cm,

Daunia Solar Cell Inc., Tozzi Renewable Energy, Mezzano, RA, Italy) are connected in a series, composed by a narrow lined and wide striped design, as shown in Figure 8.

(**a**) (**b**)

Figure 7. Set-up of the three PV vertical structures. DSSC PV wall system, made by Daunia solar cell: (**a**) assembly of 8 modules; (**b**) photograph taken during installation on the window.

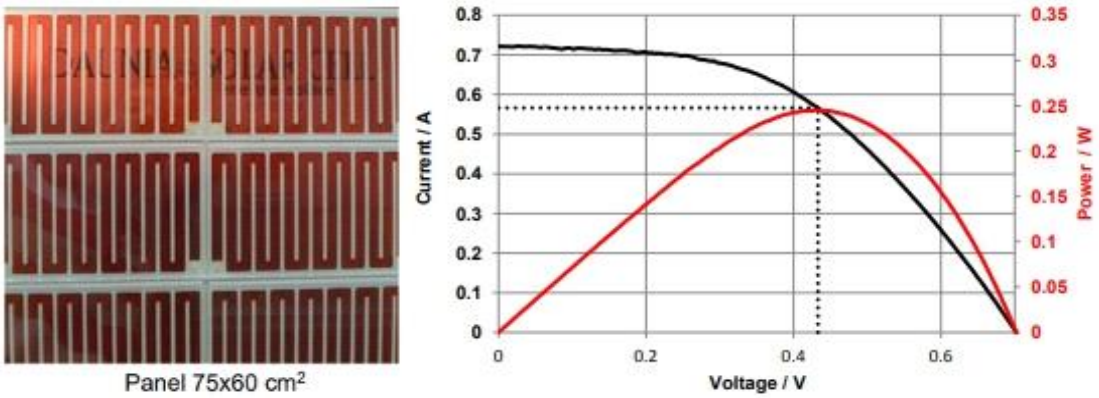

(**a**) (**b**)

Figure 8. Experimental data from Daunia solar cell prototypes, Tozzi Renewable Energy, TRE. DSSC module (area 150 cm^2) with 3% efficiency at one sun: (**a**) prototype; (**b**) graph of current and power vs voltage.

In addition to the DSSC structure, another two PV windows were taken into account (see Figure 9), composed by thin film amorphous silicon (Onyx Solar panels, Onyx Solar Energy S.L., Ávila, Spain) and with the same transparency degree.

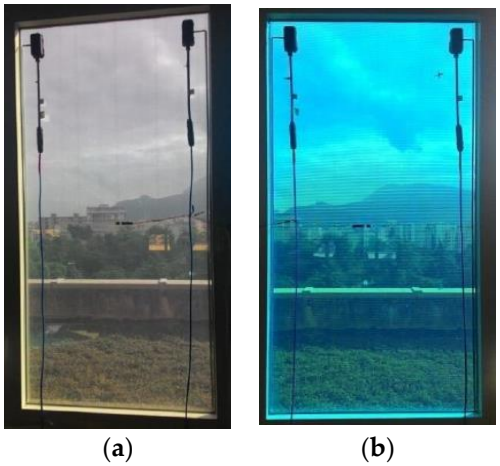

(**a**) (**b**)

Figure 9. PV wall system based on a-Si: Grey cell (**a**), Blue cell (**b**) (both made by Onyx solar).

For DDSC and a-Si PV windows, the open circuit voltages are equal respectively to 23 V and 48 V. Although these values are suitable for DC loads, they are still far from DC levels employed in DC/AC converters for domestic use. The three panels have the same size; the DSSC area has a little reduction, due to the used frames. Each vertical structure is subject to shade in the afternoon, receiving only scattered light. The DSSC is mounted inside a vertical glass block for the architectonical integration of the PV structures [21,22]. This block, which ensures transparency to radiation, is composed by two shells of transparent glass joined together with an opaque frame, as shown in Figure 10. Performances of the cells are reduced due to the adoption of such glass block, which decreases the radiation effect on the surface of the DSSC.

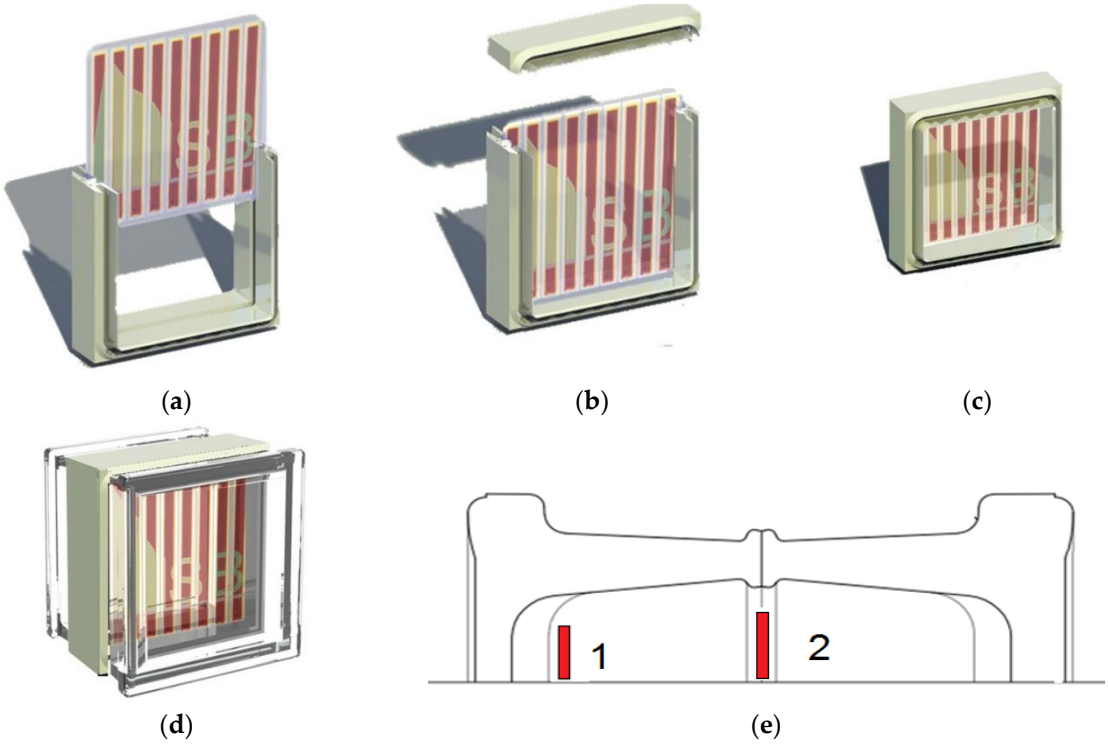

Figure 10. (**a**–**d**) Structure of the PV DSSC glass block: the opaque edging frame, two glass shell structures and the colored DSSC; (**e**) glass block section where the DSSC is colored in red: 1 internal placement on the surface, 2 in the middle section.

Performances of the proposed and described systems were experimentally evaluated by means of a measurement setup for data acquisition of currents and voltages. The test bench, whose schematic representation is shown in Figure 11, is mainly composed by: a Source-Meter (Keithley 2420, Keithley-Tektronix company, Solon, OH, USA) featuring low noise and high precision, so that a stable DC voltage can be set (12 mV source voltage accuracy, 1.5 mA measurement current accuracy); LabView® interface, to which the Source-Meter is directly connected; a homemade switch, in order to properly select which one among the three different PV vertical structures has to provide power; a pyranometer for irradiance measuring (Lafayette SPM-13: irradiance measure range: 0–1999 W/m^2, 1 W/m^2 precision; Lafayette Electronic Supply, Inc., Lafayette, IN, USA); temperature sensors (by Texas Instruments, Boulevard, Dallas, TX, USA) LM35 placed on the back of the panels (Precision Centigrade Temperature Sensors with 0.5 °C temperature accuracy); an Arduino® UNO microcontroller (Arduino S.r.l., production in Strambino, TO, Italy), which is mainly used to set measurements timing during the day and adequately control the on/off commands to the switch. The microcontroller is also connected to the Labview® interface.

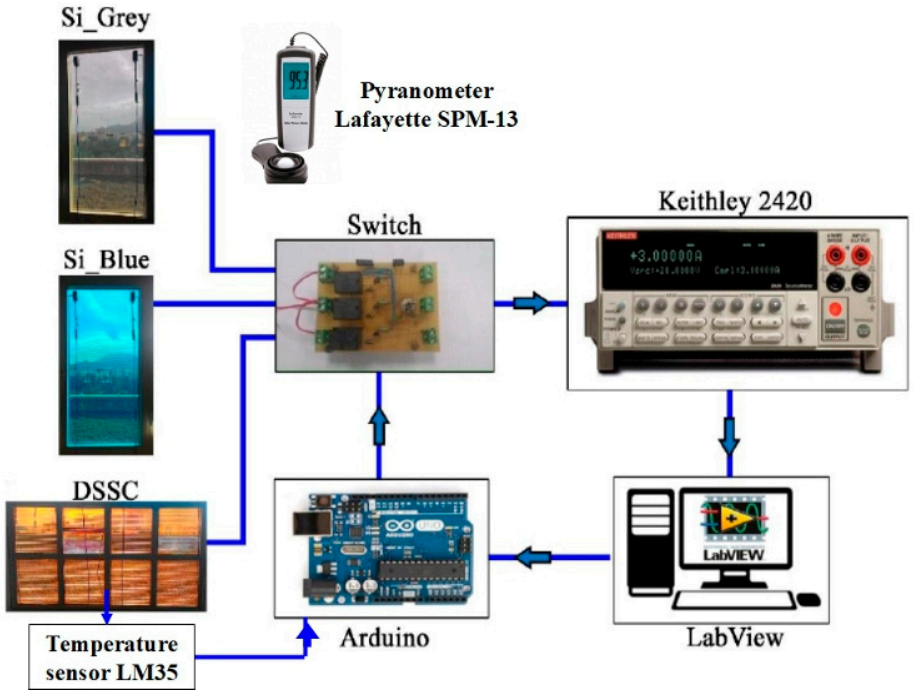

Figure 11. Test bench setup. Labview was used to acquire experimental data from Keythley 2420 (12 mV source voltage accuracy and 1.5 mA measurement current accuracy) and Arduino was used to switch the connection among the three source panels.

For each prototype, the open-circuit voltage is measured by means of the source meter and all the data are processed by the Labview® interface, which controls a cycle of measurements that starts from the open circuit voltage, decreased step-by-step until the minimum voltage level. For each module a set of measurements based on 100 acquisitions is detected, so that the voltage range is divided into 100 equal parts. The settlement of the modules is helped by delaying the acquisition system. The employment of this automated measurement system for PV modules characterization was carried out over several months. The vertical structures have been exposed towards east, so that the highest production of power is reached during the first hours of the day. In addition to electrical parameters, other significant ones, such as irradiation, glass surface and room temperatures, were detected by means of the Arduino board as well.

Characterization of the Performances of the Glass Block

In this section it was already highlighted that the adoption of the glass structure determines a performance reduction of the DSSC, shading the module during the day. Figure 12 shows the geometrical disposition of the sensors located on the surface of the glass block. The performance reduction can be computed by considering fifteen positions, taking into account also the vertical edges, whereas the sixteenth position is out of the structure, being considered as the reference value.

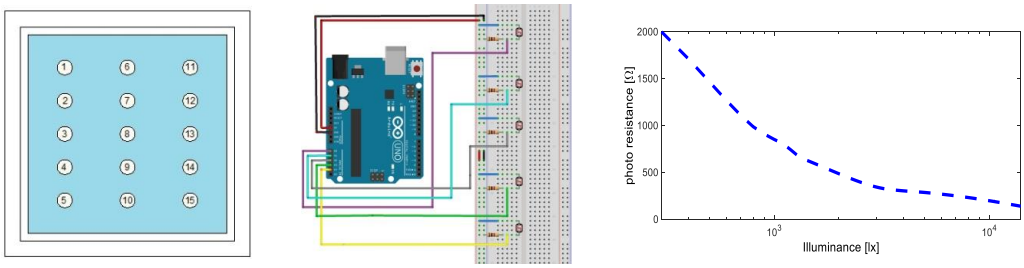

(**a**) (**b**) (**c**)

Figure 12. The fifteen positions in which the sensors were placed inside the glass block and corresponding photo-resistance and illuminance curve. Photosensitive sensor HW5P-1 Shenzhen Haiwang Sensor Co: (**a**) the used 3 × 5 matrix of photo-resistors; (**b**) Arduino scheme for the first column; (**c**) photo-resistance/illuminance curve.

Preliminary tests were provided in the laboratory: a halogen lamp illuminated the glass block with different inclinations, in order to examine the border effect, as shown in Figure 13. The daylight distribution in the glass block was performed according to four exposures: north, south, west and east [23].

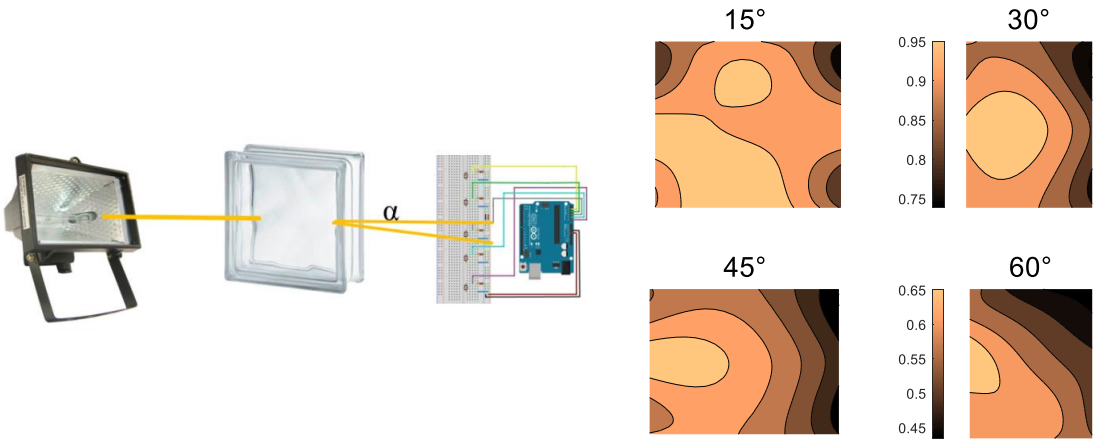

(**a**) (**b**)

Figure 13. Glass block surface shaded areas in the laboratory. Two color maps refer to the 15° and 30° inclinations, and 45° and 60° respectively. The first image shows how, by moving the position of the lamp, the effects of borders are concentrated on the edges: (**a**) scheme used for the characterization of the glass block, the angle α varies during the measurements; (**b**) evaluation of the shading in different configurations.

The cases of north and south exposures are shown in Figure 14, where the distribution of the performance reduction is highlighted as well. From this figure, clear and dark areas can be detected. For the latest, an efficiency reduction in the 10–20% range was observed, mainly when the DSSC is located in the center of the shell.

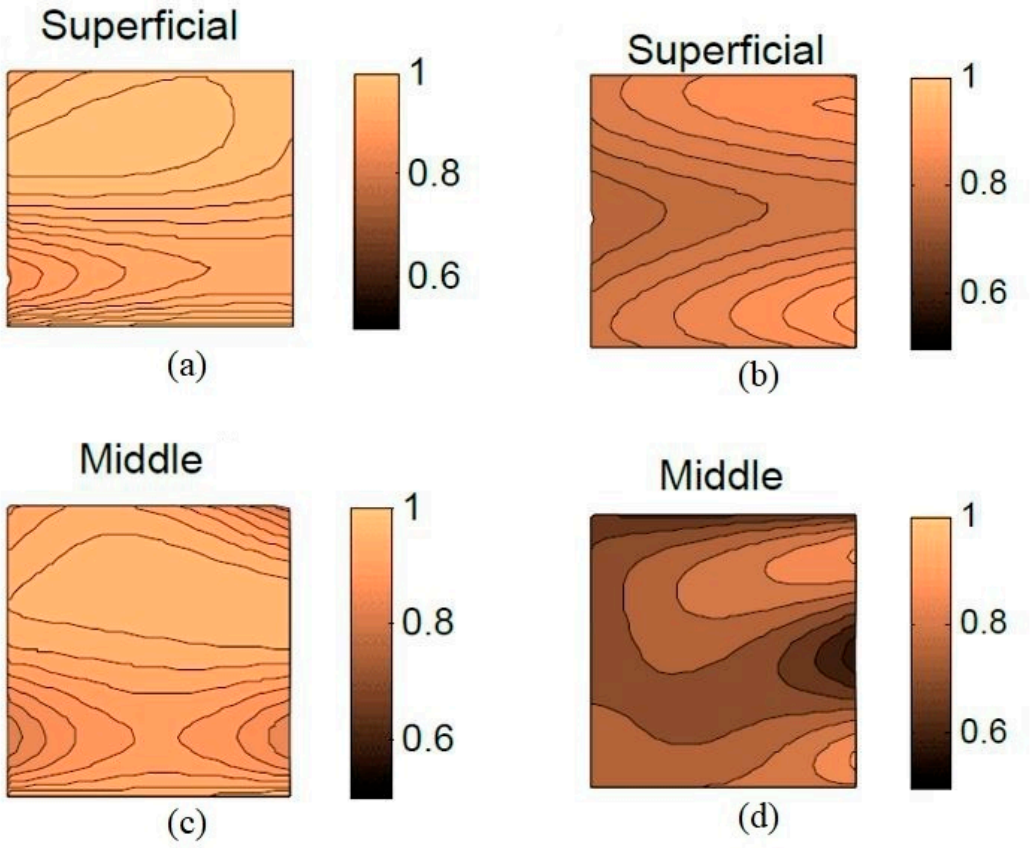

Figure 14. Glass block surface shaded areas: (**a**) and (**c**) the southern exposures; (**b**) and (**d**) the northern exposures. In (**a**) and (**b**) the measuring system is on the surface of the glass block; in (**c**) and (**d**) the measuring system is on the middle.

4. Experimental Results

By processing the experimental data obtained from the previously reported tests, I-V and P-V characteristics were determined for each proposed technology and plotted in Figures 15–20. The measured data refer to different days and different irradiance levels.

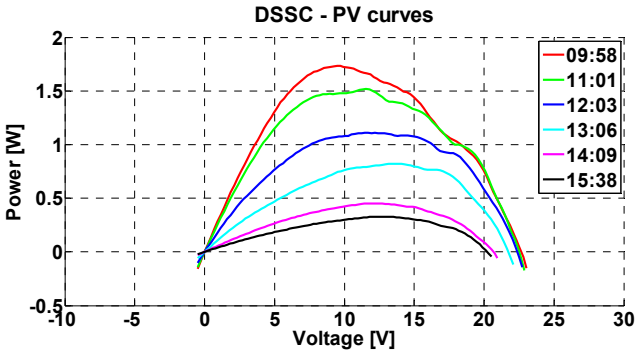

Figure 15. DSSC cell power-voltage curves for different irradiance values.

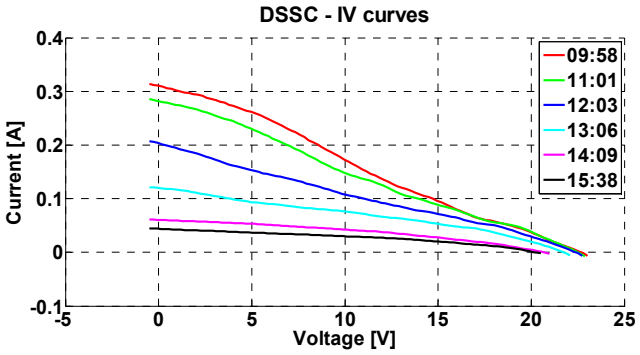

Figure 16. DSSC cell current-voltage curves for different irradiance values.

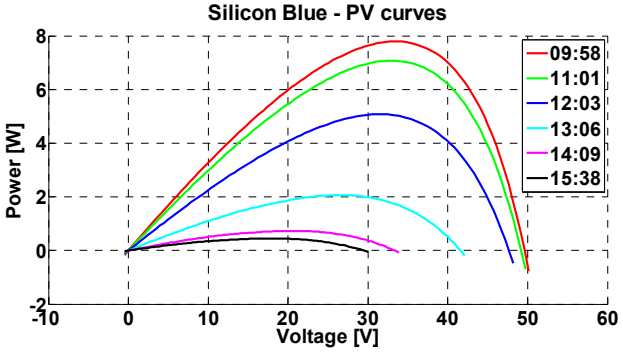

Figure 17. Blue silicon cell power-voltage curves for different irradiance values.

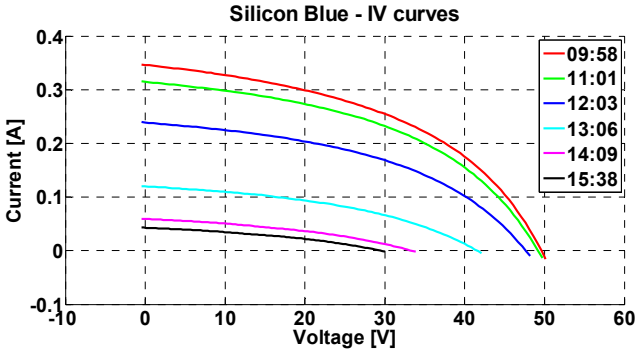

Figure 18. Blue silicon cell current-voltage curves for different irradiance values.

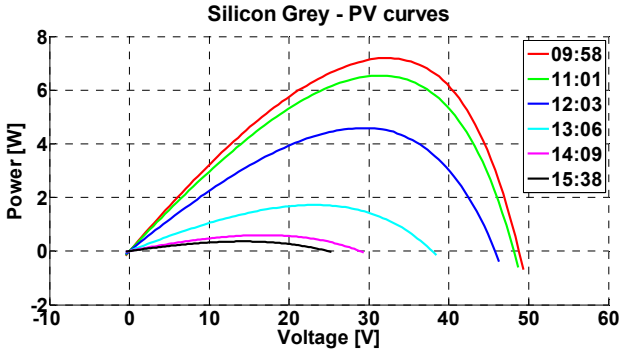

Figure 19. Grey silicon cell power-voltage curves for different irradiance values.

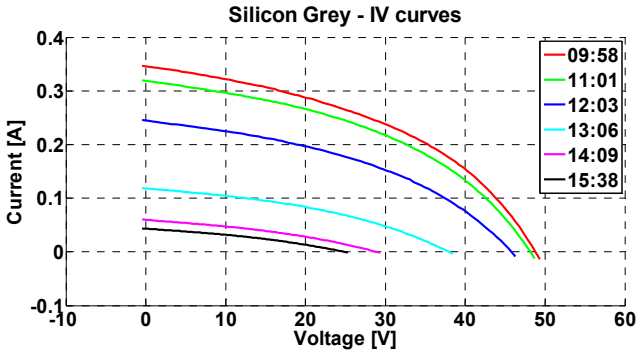

Figure 20. Grey silicon cell current-voltage curves for different irradiance values.

To gain high power output and trustworthy current-voltage curves, the measurements concern a sunny day of July with a remarkable sun radiation (1700 W/m^2 on soil surface). The values of 715 W/m^2 and 68 W/m^2 refer to the starting and final detected values of vertical irradiance, respectively. Windows belong to the Loox laboratory of University of Palermo.

The reported results show that the power produced by the DSSC module is lower than those produced by the silicon cells, which have also a higher open circuit voltage. More in particular, for the highest irradiance values the a-Si technology shows an about 50 V open circuit voltage, which is a proper value for DC power supply with respect to the 23 V presented by the DSSC generation system, which will need additional boost converters.

Comparison of the Results

Several experimental tests were carried out in order to provide a comparison among the performances achieved by the three systems in terms of produced power, efficiency and fill factor. By measuring both voltages and currents for each technology, the produced power was computed. Consequentially, the daily power profile was determined, evaluating the daily value of the maximum produced power.

The trends of the produced power during both morning and afternoon hours for each of the proposed systems are plotted in Figures 21 and 22, respectively. It can be noticed that the DSSC power is lower than the other 2 technologies during the morning. However, the values are comparable during the afternoon hours.

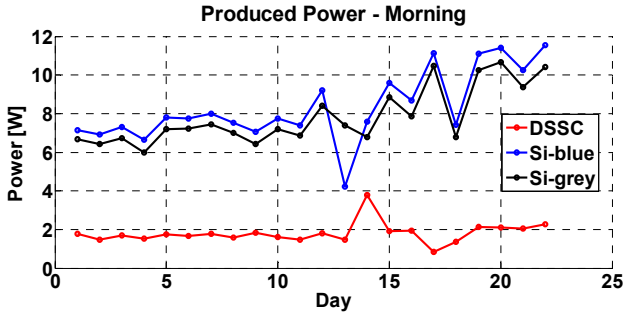

Figure 21. Morning power trends of the three generation systems.

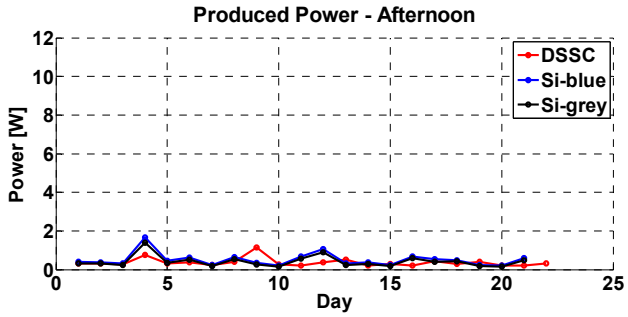

Figure 22. Afternoon power trends of the three generation systems.

It is well known that the Fill Factor (FF) characterizes the cell in terms of quality, by comparing the maximum obtainable power with the theoretical one:

$$FF = P_M/(V_{oc} \cdot I_{sc}) \quad (1)$$

where V_{oc} is the open-circuit voltage and I_{sc} is the short-circuit current. For each of the proposed systems, the FF was determined and plotted in Figures 23 and 24, which refer to morning and afternoon hours, respectively. In accordance with the previous reported trends, it can be observed that the profiles of DSSC and the Si technologies are comparable during the afternoon hours.

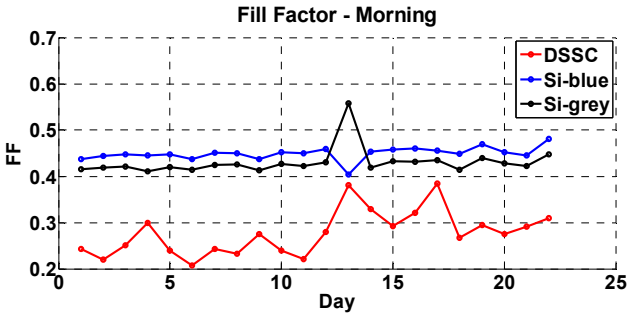

Figure 23. Morning Fill Factor (FF) trends of the three generation systems.

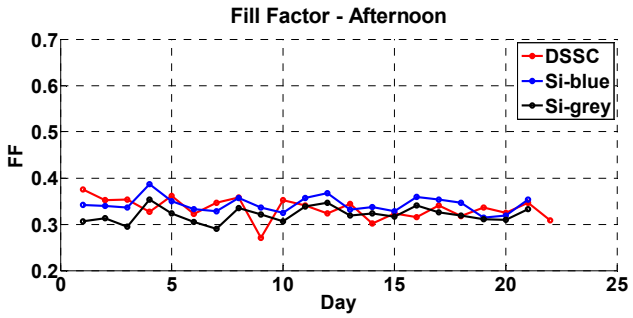

Figure 24. Afternoon FF trends of the three generation systems.

Through the following equation the efficiency is determined:

$$\eta = P_M/P_{in} = FF \times (V_{oc} \times I_{sc})/P_{in} \quad (2)$$

where P_M is the maximum power, and P_{in} is the irradiance power. The latter arises from the product between panel total area (0.72 m^2) and irradiance level.

For each of the proposed systems, the efficiency was computed and plotted in Figures 25 and 26, corresponding to the morning and to the afternoon hours, respectively. As well as for the previous

profiles, it can be noticed that the DSSC values are comparable with those obtained by the Si technology during the afternoon hours.

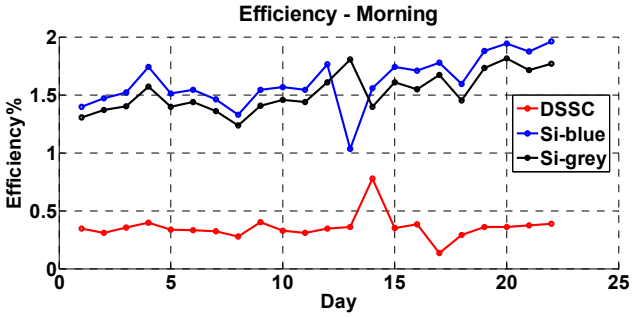

Figure 25. Efficiency profiles in the morning of the three generation systems. From the trends it is possible to remark that the Si-blue has better performances respect Si-grey, only for a particular event this trend is not verified.

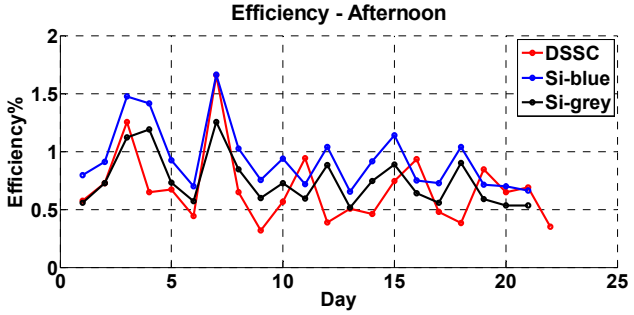

Figure 26. Efficiency profiles in the afternoon of the three generation systems.

More in detail, an efficiency in the 1–1.5% range (afternoon–morning) was measured for the Si structures, whereas the performances of the DSSC cells in diffuse light in the afternoon are improved if compared to the case of direct light in the morning. The low value of efficiency measured from the a-Si vertical structure, referred to a traditional panel (in general equal to 10% for azimuth inclination), can be explained by two factors: the first one is the vertical inclination, decreasing efficiency from its maximum value to a 0.40 factor, as reported in [24]; secondly, efficiency is further decreased due to a reduction of the active material above the glass holder, in order to gain transparency.

The experimental results obtained from the DSSC technology can be validated by considering the works presented in [10,24–26] (without taking into account the vertical disposition). More in detail, Fill Factor values found by Han et al. [10], Kwak [24], Peng [25] and Wang [27] were equal to 70%, 63%, 55.5–77.7% (depending on the color) and 55.5–73.1%, respectively (according to electrolyte properties). The DSSC performances experimentally obtained by the Authors were also confirmed by the work presented in [9].

With regards to the degradation aspects, the DSSC cell revealed a progressive color degradation, becoming even transparent during the last period of tests. This phenomenon was due to a photo-induced electrophoresis that occurred between adjacent cells and caused by the non-hermetic sealing between the strips.

However, this degradation phenomenon did not cause a significant decrease of the related electrical performances, in spite of some aesthetic alteration, as shown in Figure 27, which compares the cells throughout four months of measurements. In order to avoid this widely reported phenomenon [10,26], different efforts were addressed to the development of stable electrolytes [27].

(**a**) (**b**) (**c**)

Figure 27. Degradation of the DSSC cells: (**a**) April–May, before the measures here provided, (**b**) during July, and (**c**) after the test in September–October.

5. Discussions

This section provides a discussion in terms of both technical and economical parameters needed for the feasibility of a PV vertical structure, either with opaque panels (corresponding to the first and second generation prototypes) or with transparent windows (corresponding to the third generation prototypes). From the technical point of view, it can be noticed that the DSSC cell realization is less troublesome with respect to a traditional silicon one, mainly because of the lower number of processes needed for their fabrication. Moreover, the DSSC cells require less energy for high-temperature processes, which are only confined in the sintering process.

On the contrary, the fabrication of a silicon cell requires a relevant number of high-temperature processes, such as purification, doping and deposition of the anti-reflective coating. In addition to that, since an extremely clean working environment is required, the silicon cell production process is more complex. Therefore, by considering the previously mentioned observations, it can be stated that fabrication costs for DSSC technology should be lower than those needed for the a-Si one.

On the other hand, it must be considered that the latter is an already well-developed technology, while the DSSC has just started its evolution. As a consequence, the technologies required for the DSSC production are not fully developed in other industrial sectors. Thus, the processes are not energy-efficiently optimized in order to reduce the payback time for any investment.

From the economical point of view, the costs related to the DSSC fabrication are not easily determinable, as also reported in the recent literature. More in detail, the work proposed by Meyer [28] estimates the production costs to 2.2 \$/Wp, whereas Smestad [29] estimates their costs to 0.8 \$/Wp. This information was then updated in [30]. In terms of costs/m^2, Smestad estimated at 64 \$/m^2 (58.9 €/m^2), while Mayer computed a value equal to 110.6 \$/m^2 (101.7 €/m^2). Finally, with regards to the efficiency of the DSSC cells, Smestad suggested a value of 25%, while Mayer deducted a 5% of overall efficiency.

Although the polycrystalline silicon cell production is rapidly becoming cheaper, estimated costs for innovative structure are about 1.78 \$/Wp and 267 \$/m^2 (245.5 €/m^2). A quantitative analysis was carried out and, for this purpose, a 1.0 kWp vertical structure was considered for the related analysis. Both data reported in literature and experimentally obtained were considered for the proposed investigation.

Mayer's cell was taken into account for the DSSC comparison, since the suggested yield was the closest one, compared to that of the investigated system. Moreover, a second generation opaque a-Si panel is used as reference test, whose cost is equal to 1 €/Wp, or 150 €/m^2. Furthermore, a first generation c-Si panel for the vertical structure is considered, with cost doubled with respect to the a-Si panel.

The overall costs of vertical BIPV systems and the main parameters for a 1.0 kWp vertical structure are shown in Table 1. The cheapest technology is not applicable to a window, being based on the opaque amorphous silicon panel. As far as the Mayer's cell (M DSSC) is concerned, although its cost is similar to the conventional opaque panel, the efficiency values given by the experimentally evaluated systems are still far from the theoretical ones.

Table 1. Main parameters for 1.0 kWp vertical integrated systems.

	Experimental		Technical Literature		
	DSSC	**Blue/grey**	**M DSSC**	**c-Si**	**a-Si**
Horizontal Efficiency [%]			5%	16%	10%
Vertical Efficiency [%]	0.31%	1.31%	2.5%	6.4%	4%
Surface [m^2]	322	76.6	40	17	25
Cost [€]	32,806	18,740	4068	5100	3750
Glass block [€]	36,452		4520		

The system realization costs are slightly increased by the employment of a glass block, due to the yield reduction because of the shade of the frames [23]. From Table 1 it appears evident that the effectiveness of the productivity for the innovative vertical structures is strictly dependent on its extremely accurate design, by also considering the optimal exposure of the solar panels.

The DSSC technology is suitable for the realization of transparent windows, in order to provide indoor lighting for the related environments. However, the adoption of this transparent technology leads to technically poorer performances and higher costs and spaces, if compared with those obtained with opaque panels, such as c-Si or a-Si.

By referring to [31], green buildings provide increased water and energy efficiency, reduced consumption of natural and material resources, as well as improved health for human and environment. However, no mention was addressed in terms of costs. Therefore, the proposed work could be an important aid for the discussion and support to the thesis of a green building cost premium [32], even though further research on BIPV technology must be accurately developed [33–39].

6. Conclusions

This paper presented an experimental investigation on the performances of solar generating vertical structures, leading also to their technical and economical comparison. DSSC and a-Si thin film solar windows were compared, experimentally testing three systems, such as DSSC and blue and grey solar cells.

It should be emphasized that the photovoltaic window does not aim at replacement of normal photovoltaic systems (azimuth inclined). The idea presented in [40] consisted in smart windows exceeding the traditional window. On the other hand, as stated in [41], smart windows will be characterized also for other several advantages offered, if compared to traditional ones, with a neat money saving for air-conditioning, heating, lighting, and curtains.

The electrical power generated during several hours of a day by each of the PV vertical structures was measured, as well as the fill factor and related efficiency. The performance comparison between the proposed systems determined a higher power production and efficiency by the silicon cells among the daily hours. Nevertheless, during the hours of late afternoon under scattered light conditions, the performances given by the DSSC cells were almost comparable with the silicon ones.

Thus, it can be stated that the three technologies proposed in this work, even if their performances are still far from satisfying the power requests, exhibited an adequate degree of architectural integration in buildings. In such a way, the main objective, as previously explained, is not to feed the building but to create an energy harvesting [42].

Author Contributions: The authors have contributed equally to this work. The authors of this manuscript jointly have conceived the theoretical analysis, modeling, simulation and obtained the experimental data.

Funding: This work was financially supported by LEAP (Laboratory of Electrical Applications of the University of Palermo), by LOOX (Laboratory of Optics and OptoelectroniX) of the University of Palermo.

Conflicts of Interest: The authors declare no conflict of interest.

References

1. Directive 2010/31/EU of the European Parliament and of the Council on the Energy Performance of Buildings. Available online: https://eur-lex.europa.eu/LexUriServ/LexUriServ.do?uri=OJ:L:2010:153:0013:0035:EN:PDF (accessed on 29 July 2019).
2. Cornaro, C.; Bartocci, S.; Musella, D.; Strati, C.; Lanuti, A.; Mastroianni, S.; Penna, S.; Guidobaldi, A.; Giordano, F.; Petrolati, E.; et al. Comparative analysis of the outdoor performance of a dye solar cell mini-panel for building integrated photovoltaics applications. *Prog. Photovolt.* **2015**, *23*, 215–225. [CrossRef]
3. Cornaro, C.; Renzi, L.; Pierro, M.; Di Carlo, A.; Guglielmotti, A. Thermal and Electrical Characterization of a Semi-Transparent Dye-Sensitized Photovoltaic Module under Real Operating Conditions. *Energies* **2018**, *11*, 155. [CrossRef]
4. Passer, A.; Ouellet-Plamondon, C.; Kenneally, P.; John, V.; Habert, G. The impact of future scenarios on building refurbishment strategies towards plus energy buildings. *Energy Build.* **2016**, *124*, 153–163. [CrossRef]
5. Chow, T.-T.; Li, C.; Lin, Z. Innovative solar windows for cooling-demand climate. *Sol. Energy Mater. Sol. Cells* **2010**, *94*, 212–220. [CrossRef]
6. Song, J.-W.; An, Y.-S.; Kim, S.-G.; Lee, S.-J.; Yoon, J.-H.; Choung, Y.-K. Power output analysis of transparent thin-film module in building integrated photovoltaic system (BIPV). *Energy Build.* **2018**, *40*, 2067–2075. [CrossRef]
7. O'Reagan, B.; Grätzel, M. A low-cost, high-efficiency solar cell based on dye-sensitized colloidal TiO_2 films. *Nature* **1991**, *353*, 737–740. [CrossRef]
8. Shukla, A.K.; Sudhakar, K.; Baredar, P. A comprehensive review on design of building integrated photovoltaic system. *Energy Build.* **2016**, *128*, 99–110. [CrossRef]
9. Hinsch, A.; Brandt, H.; Veurman, W.; Hemming, S.; Nittel, M.; Würfel, U.; Putyra, P.; Lang-Koetz, C.; Stabe, M.; Beucker, S.; et al. Dye solar modules for facade applications: Recent results from project ColorSol. *Sol. Energy Mater. Sol. Cells* **2009**, *93*, 820–824. [CrossRef]
10. Han, C.; Park, S.; Oh, W. Reliability-based structural optimization of 300 × 300 mm^2 dye-sensitized solar cell module. *Sol. Energy* **2017**, *150*, 128–135. [CrossRef]
11. Laudani, A.; Riganti-Fulginei, F.; Salvini, A.; Parisi, A.; Pernice, R.; Ricco-Galluzzo, F.; Cino, A.C.; Busacca, A.C. One diode circuital model of light soaking phenomena in Dye-Sensitized Solar Cells. *Optik* **2018**, *156*, 311–317. [CrossRef]
12. Parisi, A.; Pernice, R.; Andò, A.; Cino, A.C.; Franzitta, V.; Busacca, A.C. Electro-optical characterization of ruthenium-based dye sensitized solar cells: A study of light soaking, ageing and temperature effects. *Optik* **2017**, *135*, 227–237. [CrossRef]
13. Parisi, A.; Pernice, R.; Adamo, G.; Miceli, R.; Ricco Galluzzo, F.; Cino, A.C.; Busacca, A.C. Anomalous electrical parameters improvement in Ruthenium DSSC. In Proceedings of the 13th International Conference on Ecological Vehicles and Renewable Energies (EVER), Monte-Carlo, Monaco, 10–12 April 2018.
14. Parisi, A.; Pernice, R.; Adamo, G.; Cino, A.C. Numerical analysis of light soaking phenomenon in Ruthenium Based Dye Sensitized Solar Cells. In Proceedings of the 6th International Conference on Clean Electrical Power (ICCEP2017), Santa Margherita Ligure, Italy, 27–29 June 2017; pp. 773–777.
15. Adamo, G.; Parisi, A.; Pernice, R.; Ricco Galluzzo, F.; Di Noia, L.; Cino, A.C. Laser Beam Induced Current measurements on Dye Sensitized Solar Cells and Thin Film Cig (S, Se) 2 modules. In Proceedings of the 6th International Conference on Clean Electrical Power (ICCEP2017), Santa Margherita Ligure, Italy, 27–29 June 2017.
16. Parisi, A.; Pernice, R.; Adamo, G.; Miceli, R.; Cino, A.C. Anomalous Performance Enhancement Effects in Ruthenium-Based Dye Sensitized Solar Cells. In Proceedings of the 6th International Conference on Clean Electrical Power (ICCEP2017), Santa Margherita Ligure, Italy, 27–29 June 2017; pp. 174–178.
17. Green, M.A.; Hishikawa, Y.; Dunlop, E.D.; Levi, D.H.; Hohl-Ebinger, J. Solar cell efficiency tables (Version 53). *Prog. Photovolt. Res. Appl.* **2019**, *27*, 3–12. [CrossRef]
18. Lee, J.W.; Park, J.; Jung, H.-J. A feasibility study on a building's window system based on dye-sensitized solar cells. *Energy Build.* **2014**, *81*, 38–47. [CrossRef]
19. Skandalos, N.; Karamanis, D. Investigation of thermal performance of semi-transparent PV technologies. *Energy Build.* **2016**, *124*, 19–34. [CrossRef]
20. Skandalos, N.; Karamanis, D. PV glazing technologies. *Renew. Sust. Energy Rev.* **2015**, *49*, 306–322. [CrossRef]
21. Yoon, S.; Tak, S.; Kim, J.; Jun, Y.; Kang, K.; Park, J. Application of transparent dye-sensitized solar cells to building integrated photovoltaic systems. *Build. Environ.* **2011**, *46*, 1899–1904. [CrossRef]

22. Corrao, R.; Morini, M. Integration of Dye-Sensitized Solar Cells with Glassblock. *Czas. Tech.* **2012**, *3*, 55–64.
23. Viola, F.; Romano, P.; Miceli, R.; Riva Sanseverino, E.; Corrao, R.; Morini, M.; Pastore, L.; Pidanic, J.; Perrone, G. Performance of the Glass Block in Photovoltaic Generation. In Proceedings of the 2015 10th International Conference on Ecological Vehicles and Renewable Energies (EVER), Monte Carlo, Monaco, 31 March–2 April 2015.
24. Kwak, C.-H.; Baeg, J.-H.; Yang, I.-M.; Giribabu, K.; Lee, S.; Huh, Y.-S. Degradation analysis of dye-sensitized solar cell module consisting of 22 unit cells for thermal stability: Raman spectroscopy study. *Sol. Energy* **2016**, *130*, 244–249. [CrossRef]
25. Peng, M.; Dong, B.; Cai, X.; Wang, W.; Jiang, X.; Wang, Y.; Yang, Y.; Zou, D. Organic dye-sensitized photovoltaic fibers. *Sol. Energy* **2017**, *150*, 161–165. [CrossRef]
26. Sastrawan, R. Photovoltaic Modules of Dye Solar Cells. Ph.D. Thesis, Freiburg University, Freiburg, Germany, 2006.
27. Wang, Y.-H.; Wong, D.S.-H. Modelling accelerated degradation test and shelf-life prediction of dye-sensitized solar cells with different types of solvents. *Sol. Energy* **2015**, *118*, 600–610. [CrossRef]
28. Meyer, T.; Gratzel, M. Solid State Nanocrystalline Titanium Oxide Photovoltaic Cells. Available online: https://infoscience.epfl.ch/record/32019/files/EPFL_TH1542.pdf (accessed on 29 July 2019).
29. Smestad, G. Testing of dye-sensitized TiO_2 solar cells I & II. *Sol. Energy Mater. Sol. Cells* **1994**, *32*, 259–272.
30. Kalowekamo, J.; Baker, E. Estimating the manufacturing cost of purely organic solar cells. *Sol. Energy* **2009**, *83*, 1224–1231. [CrossRef]
31. Laustsen, J. *Energy Efficiency Requirements in Building Codes and Energy Efficiency Policies for New Buildings*; International Energy Agency (IEA): Paris, France, 2008.
32. Dwaikat, L.-N.; Ali, K.N. Green buildings cost premium: A review of empirical evidence. *Energy Build.* **2016**, *110*, 396–403. [CrossRef]
33. Liu, Q.; Gao, N.; Liu, D.; Liu, J.; Li, Y. Structure and Photoelectrical Properties of Natural Photoactive Dyes for Solar Cells. *Appl. Sci.* **2018**, *8*, 1697. [CrossRef]
34. Al-Attafi, K.; Nattestad, A.; Dou, S.X.; Kim, J.H. A Comparative Study of TiO_2 Paste Preparation Methods Using Solvothermally Synthesised Anatase Nanoparticles in Dye-Sensitised Solar Cells. *Appl. Sci.* **2019**, *9*, 979. [CrossRef]
35. Kolawole, S.Y.; Tesleem, A.B.; Kazeem, A.A. Optimization of TiO_2 Based Henna Dye Sensitized Solar Cell using Grey-Taguchi Technique. *Int. J. Renew. Energy Res.* **2016**, *6*, 1119–1128.
36. Saha, S.; Das, P.; Chakraborty, A.K.; Sarkar, S.; Debbarma, R. Fabrication of DSSC with nanoporous TiO_2 film and Kenaf Hibiscus dye as sensitizer. *Int. J. Renew. Energy Res.* **2016**, *6*, 620–627.
37. Toufik, A. The Gouy-Chapman capacitor of double layer in Dye Sensitized Solar Cells: Study and simulation. *Int. J. Renew. Energy Res.* **2016**, *6*, 164–170.
38. Viola, F.; Romano, P.; Miceli, R.; Spataro, C.; Schettino, G.; Caruso, M.; Busacca, A.; Parisi, A.; Guarino, S.; Cino, A. Comparison on the use of PV systems in the vertical walls. In Proceedings of the 2015 International Conference on Renewable Energy Research and Applications (ICRERA), Palermo, Italy, 22–25 November 2015.
39. Acciari, G.; Busacca, A.; Guarino, S.; Imburgia, A.; Madonia, A.; Miceli, R.; Parisi, A.; Sanseverino, E.R.; Romano, P.; Sauba, G.; et al. PV systems in the vertical walls: A comparison of innovative structures. In Proceedings of the 2016 International Conference on Renewable Energy Research and Applications (ICRERA), Birmingham, UK, 20–23 November 2016; pp. 1185–1190.
40. Bella, F.; Leftheriotis, G.; Griffini, G.; Syrrokostas, G.; Turri, S.; Grätzel, M.; Gerbaldi, C. A New Design Paradigm for Smart Windows: Photocurable Polymers for Quasi-Solid Photoelectrochromic Devices with Excellent Long-Term Stability under Real Outdoor Operating Conditions. *Adv. Funct. Mater.* **2016**, *26*, 1127–1137. [CrossRef]
41. Amasawa, E.; Sasagawa, N.; Kimura, M.; Taya, M. Design of a New Energy-Harvesting Electrochromic Window Based on an Organic Polymeric Dye, a Cobalt Couple, and PProDOT-Me_2. *Adv. Energy Mater.* **2014**, *4*, 1400379. [CrossRef]
42. Vasiliev, M.; Alameh, K.; Nur-E-Alam, M. Spectrally-Selective Energy-Harvesting Solar Windows for Public Infrastructure Applications. *Appl. Sci.* **2018**, *8*, 849. [CrossRef]